Electromagnetic shocks on the optical cycle of ultrashort pulses in triple-resonance Lorentz dielectric media with subfemtosecond nonlinear electronic Debye relaxation

L. Gilles,* J. V. Moloney,† and L. Vázquez
Escuela Superior de Informática, Departamento de Matemática Aplicada, Universidad Complutense, E-28040 Madrid, Spain
(Received 8 February 1999)

The dynamical evolution of an intense ultrashort sub-10-fs two-cycle optical pulse is considered as it propagates through a transparent third-order dielectric medium characterized by three resonance lines and a finite sub-fs relaxation time of the electronic nonlinearity. Numerical integration of the full Maxwell's equations incorporating triple-resonance Lorentz linear dispersion and Debye nonlinear dispersion, for a linearly polarized electromagnetic pulse centered at $\lambda_0 = 1.24\,\mu$m in the normal dispersion region near the zero dispersion wavelength, shows the formation of *shocks occurring on the optical cycle* due to the generation of optical harmonics. The finite relaxation time of the nonlinear electronic response (sub-fs time scale) (i) slows down the steepening rate of the optical cycle; (ii) does not limit the generation of strongly phase matched optical harmonics, and consequently the development of infinitely sharp edges on the optical cycle producing its breaking when linear dispersion is not included; (iii) reduces the production of phase matched harmonics and consequently the sharpening of the jumps when dispersion is present, compared to the case of an instantaneous nonlinear response; and (iv) reduces the harmonic spectrum spreading and modulation at later times on the appearance of self-steepening of the electric field envelope. [S1063-651X(99)13107-6]

PACS number(s): 42.65.Ky

I. INTRODUCTION

Advances in ultrashort pulse laser technology have made possible the generation of light pulses carrying a substantial part of their energy in only a few optical cycles [1,2]. Electromagnetic energy compressed in brief time intervals permits one to achieve extremely high peak powers. Coherent light pulses with multiterrawatt peak power of energy at the joule level are now available, opening new exciting opportunities in the research of high field nonlinear phenomena. They may be used in time-resolved spectroscopic techniques to study transient chemical processes on the fs time scale, e.g., dissociation, or for quantum control of chemical bonding [3]. Ultrashort pulses could also find wide applications in imaging, medical IR tomography [4].

Recently, the concept of decomposing the wave packet into a carrier wave and an envelope has been shown to be legitimate down to the single-cycle [full width at intensity half maximum, (FWHM)] regime and a fundamental three-dimensional (3D) envelope propagation equation based on this framework has been derived by Brabec and Krausz (BK) [5]. In this framework, not only the envelope phase but also the *carrier phase* must not vary significantly as the pulse covers a distance equal to the carrier wavelength [the so called slowly evolving wave approximation]. On the other hand, it does not impose a limitation on the pulse width. In the specific case of 1D propagation (i.e., when diffraction may be discarded), the BK equation reduces to a generalized nonlinear Schrödinger equation derived by Blow and Wood [6], which may be written as

$$i\frac{\partial A}{\partial x} + i\beta_1\frac{\partial A}{\partial t} + \hat{L}A + \gamma\left(1 + \frac{i}{\omega_0}\frac{\partial}{\partial t}\right)\left[A\int_{-\infty}^{t}\chi^{(3)}(t-t_1)|A(x,t_1)|^2 dt_1\right] = 0, \tag{1}$$

where the linear propagation operator $\hat{L}$ describing the linear losses and higher-order dispersion effects is given by

$$\hat{L} = i\frac{\alpha_0}{2} - \frac{\alpha_1}{2}\frac{\partial}{\partial t} + \sum_{m=2}^{\infty}\frac{\beta_m + (i/2)\alpha_m}{m!}\left(i\frac{\partial}{\partial t}\right)^m, \tag{2}$$

with

$$\beta_m = \mathrm{Re}(\partial^m k/\partial\omega^m)_{\omega_0}, \quad \alpha_m = 2\,\mathrm{Im}(\partial^m k/\partial\omega^m)_{\omega_0}, \tag{3}$$

and

$$\gamma = \frac{n_2\omega_0}{c}. \tag{4}$$

Far from resonances (parametric processes, i.e., the initial and final quantum states of the medium are identical), $\alpha_m = 0$ $(m = 0,1,2,3,...)$. Near resonances (nonparametric pro-

*Electronic address: fitelz2@sis.ucm.es
†Present address: Arizona Center for Mathematical Sciences, Department of Mathematics, University of Arizona, Tucson, AZ 85721.

cesses, i.e., population transfer between energy levels), $\alpha_m \neq 0$. The operator $[1+(i/\omega_0)(\partial/\partial t)]$ in Eq. (1) gives rise to the *envelope* shock (self-steepening), a nonlinear higher-order effect resulting from the intensity dependence of the group velocity, while the memory integral describes the delayed intensity response. Two different types of physical mechanisms contribute to the nonlinear third-order electric susceptibility far from resonance and contribute additively to $\chi^{(3)}$ [7]. An electronic contribution, nearly instantaneous ($\tau \sim 0.1-0.5$ fs, where τ is the relaxation time) arising from the electronic response to the applied electric field against the heavy nuclei considered fixed at an average position. The second, nuclear contribution (Raman self-scattering), arises from the electric field induced changes in the internal nuclear vibrations on a much longer time scale ($\sim$100 fs), and are usually temperature dependent.

Raman self-scattering produces in the context of optical solitons a continuous downshift (redshift) of the soliton carrier frequency, a phenomenon know as soliton self-frequency shift [8], and consequently, in the anomalous dispersion regime, a continuous deceleration of the pulse. Since its experimental discovery [9], numerical and experimental [10,11] investigations of higher-order nonlinear effects resulting from the finite response time of the Raman nonlinearity have been carried out extensively because of their fundamental as well as technological importance.

In this paper, numerical integration of the full Maxwell's equations for linearly polarized fields in one space dimension using the finite-difference time-domain (FDTD) method [12,13] is performed to investigate the effects of the *finite nonlinear sub-fs electronic relaxation* on the formation and dynamical evolution of *shocks on the optical cycle* of a sub-10-fs pulse containing only two oscillation cycles (FWHM) traveling in the normal dispersion region of the host material. These electromagnetic shocks in the optical range occur due to the generation of optical harmonics, the time (distance) of shock formation being directly related to the third harmonic period (wavelength) in the instantaneous nonlinear response limit.

The possibility of observing self-steepening of optical pulses and the formation of shocks on the *envelope* has been extensively discussed [1]. Raman-induced optical shocks and kink solitons representing shock fronts propagating undistorded inside optical fibers have also been predicted [14] in both the anomalous and normal dispersion regimes, although they are unstable because of the inherent modulation instability of the cw background. Stable dark shock waves in dissipative Schrödinger systems have also been demonstrated [15].

In contrast with the former envelope shock phenomena, the formation of shocks occurring on the optical carrier wave has received little attention. Electromagnetic shocks (discontinuity of the electric and magnetic fields) and shock wave trains of intense linearly polarized radiation were conjectured theoretically in 1965 by Rosen [16] who emphasized the rigorous correspondence between the theory of electromagnetic shocks and that of large amplitude 1D pressure waves in solids. Recently, the authors of Ref. [17] discussed carrier shocking for a single-resonance Lorentz medium with instantaneous nonlinear response. The aim of this paper is to generalize their analysis to the more physically realistic case of a multiple-resonance Lorentz transparent medium, and to analyze the influence of the delayed sub-fs nonlinear electronic response on the generation of optical harmonics and therefore on the shocks occurring on the optical cycle. Although the response of nonlinearities in electronic polarization is very rapid, relaxation should be taken into account for ultrashort pulses containing only a few cycles. Shocks on the optical cycle cannot easily be developed in real media because of group velocity dispersion (GVD). Phase velocity mismatch leads to the separation of the optical harmonics from the main pulse traveling at a different group velocity, and hence limits the steepening on the optical cycle. Interferometric fringe autocorrelation techniques may provide direct measurement of the optical cycle [18], and thus carrier shock formation. Good candidate materials to observe carrier shocks should have a large nonlinear index of refraction n_2 and a broad spectral region of small dispersion where the phase to group velocity v_p/v_g is close to unity. For illustrative purposes we have chosen fused silica (SiO_2) as dispersive nonlinear dielectric material due to its considerable importance in optical communications and good dispersion properties around the zero dispersion point $\lambda_{ZDP}=1.27\,\mu$m. Maxwell's equations were solved for the evolution of an initial hyperbolic secant electric field envelope of duration equal to $\tau_p=8.8$ fs (FWHM) (time constant $t_0=\tau_p/[2\ln(1+\sqrt{2})]=5$ fs), and a peak intensity equal to the estimated silica damage threshold intensity in the sub-10-fs regime $I_0=50\,\mathrm{TW/cm^2}$. Fused silica is characterized by three absorption bands (two bands in the vacuum UV and one band in the middle IR) and a nonlinear index change at the peak of the pulse $\delta n=n_2 I_0\sim 1.5\%$. The index of refraction is given by $n=n_0+\delta n$, and $\delta n/n_0\sim 1\%$ can be obtained. Far from these three resonances, bulk fused silica is well approximated by the Sellmeier dispersion relation [19] covering both normal and anomalous dispersion regimes. At the pulse center vacuum wavelength $\lambda_0=1.24\,\mu$m (a spectral FWHM of $\Delta\lambda\sim 200$ nm) ($\omega_0=1520$ THz and $\Delta\omega\sim 224$ THz), the second-order (GVD) is only $k_0''=2.83\,\mathrm{ps^2/km}$.

To minimize the effects of dispersion, known to play a crucial role in shock formation, leading to shock dissipation [1], carrier shock wave is best evidenced close to the zero dispersion wavelength, where the phase and group velocity mismatch is minimum. At the pulse center wavelength $\lambda_0=1.24\,\mu$m, the phase-group velocity ratio $v_p/v_g\sim 1$. In this small dispersion limit, part of the third-harmonic pulse generated by the Kerr nonlinearity copropagates with the fundamental and is thus phase matched. For the chosen pulse parameters the dispersion length $L_D^{(2)}=\tau_p^2/k_0''\sim 2.7$ cm, which is much greater than the nonlinear length scale $L_{NL}=1/(\gamma I_0)=c/(\omega_0 n_2 I_0)=\lambda_0/(2\pi n_2 I_0)\sim 10.6\lambda_0\sim 8.7 c t_0$, and hence shocks on the optical cycle can occur over propagation distances of a few micrometers.

II. MODEL SYSTEM

Maxwell's equations for the electric and magnetic field quantities **E** and **H** in a nonmagnetic dielectric medium with no free charges are

$$\nabla\times\mathbf{E}=-\mu_0\partial\mathbf{H}/\partial t,$$

$$\nabla\times\mathbf{H}=\partial\mathbf{D}/\partial t. \tag{5}$$

The material linear and nonlinear responses are included through the constitutive relation $\mathbf{D}=\epsilon_0[\mathbf{E}+\mathbf{\Phi}^{\rm tot}]$, where $\mathbf{\Phi}^{\rm tot}=\mathbf{\Phi}^{(1)}+\mathbf{\Phi}^{(3)}$, is the total induced electric macroscopic polarization, consisting of linear and nonlinear parts. The triple-resonance Lorentz oscillator is represented by the convolution integral

$$\mathbf{\Phi}^{(1)}(t)=\sum_{j=1}^{3}\mathbf{\Phi}_j^{(1)}(t)=\int_{-\infty}^{t}\chi^{(1)}(t-t_1)\mathbf{E}(t_1)dt_1, \quad (6)$$

with the linear susceptibility given by

$$\chi^{(1)}(t)=\sum_{j=1}^{3}\chi_j^{(1)}(t),$$
$$\chi_j^{(1)}(t)=\frac{\beta_j\omega_j^2}{\Omega_j}\exp(-\gamma_j t)\sin(\Omega_j t)\Theta(t), \quad (7)$$

where $\Omega_j=\sqrt{\omega_j^2-\gamma_j^2}$. Here ω_j is the undamped resonance frequency of the jth resonance line ($j=1$, 2, and 3), β_j is the strength of the resonance, and γ_j is the phenomenological damping constant. For simplicity, a centrosymmetric and isotropic material has been assumed, so that the different susceptibility tensors are scalar quantities, i.e., $\chi^{(1)}=\chi_{yy}^{(1)}=\chi_{zz}^{(1)}$. Relaxation of the nonlinear response of the medium is taken into account phenomenologically through a Debye model

$$\mathbf{\Phi}^{(3)}(t)=a\mathcal{Q}(t)\mathbf{E}(t),$$
$$\mathcal{Q}(t)=\int_{-\infty}^{t}\chi^{(3)}(t-t_1)\|\mathbf{E}(t_1)\|^2dt_1,$$
$$\chi^{(3)}(t)=\frac{1}{\tau}\exp(-t/\tau), \quad (8)$$
$$\int_{-\infty}^{\infty}\chi^{(3)}(t)dt=1,$$

where a is the third-order nonlinear coupling constant. We have also assumed that $\chi^{(3)}=\chi_{yyyy}^{(3)}=\chi_{zzzz}^{(3)}$, and that the second-order susceptibility tensor $\chi^{(2)}$ is identically zero [20]. As a consequence of isotropy, the electric induction field **D** and the electric field **E** are parallel. The third-order nonlinear polarization reduces to the instantaneous intensity-dependent Kerr response in the limit of infinitely fast response ($\tau\to 0$).

We restrict our attention to electromagnetic plane waves linearly polarized propagating along the x axis, in which case Maxwell's equations (5) are

$$\frac{\partial}{\partial t}H=\frac{1}{\mu_0}\frac{\partial}{\partial x}E,$$
$$\frac{\partial}{\partial t}D=\frac{\partial}{\partial x}H, \quad (9)$$
$$D=\epsilon_0[E+\Phi^{(1)}+\Phi^{(3)}],$$

where $H=H_y$, $E=E_z$, $D=D_z$. Decomposed into envelope and carrier waves, the electromagnetic fields take the form

$$\begin{bmatrix}E(x,t)\\H(x,t)\\D(x,t)\end{bmatrix}=\frac{1}{2}\begin{bmatrix}E_0q(x,t)\\H_0h(x,t)\\D_0d(x,t)\end{bmatrix}\exp[i(k_0x-\omega_0t)]+\text{C.c.} \quad (10)$$

In terms of the temporal Fourier transform,

$$E(t)=\frac{1}{2\pi}\int_{-\infty}^{\infty}\hat{E}(\omega)\exp(i\omega t)d\omega,$$
$$\hat{E}(\omega)=\int_{-\infty}^{\infty}E(t)\exp(-i\omega t)dt, \quad (11)$$

the medium polarizations are written as

$$\hat{\Phi}^{(1)}(\omega)=\hat{\chi}^{(1)}(\omega)\hat{E}(\omega),$$
$$\hat{\chi}^{(1)}=\sum_{j=1}^{3}\frac{\beta_j\omega_j^2}{\omega_j^2-\omega^2-2i\gamma_j\omega},$$
$$\hat{\Phi}^{(3)}(\omega)=a\int_{-\infty}^{\infty}\hat{\mathcal{Q}}(\omega-\omega_0)\hat{\mathbf{E}}(\omega_0)d\omega_0,$$
$$\hat{\mathcal{Q}}(\omega-\omega_0)=\hat{\chi}^{(3)}(\omega-\omega_0)\int_{-\infty}^{\infty}\hat{\mathbf{E}}(\Omega+\omega-\omega_0)$$
$$\cdot\hat{\mathbf{E}}^*(\Omega-\omega+\omega_0)d\Omega, \quad (12)$$
$$\hat{\chi}^{(3)}(\omega-\omega_0)=\frac{1-i(\omega-\omega_0)\tau}{1+(\omega-\omega_0)^2\tau^2}. \quad (13)$$

In the time domain, Eqs. (9) are equivalently expressed in the form of a wave equation

$$\frac{\partial^2}{\partial t^2}E-c^2\frac{\partial^2}{\partial x^2}E+\frac{\partial^2}{\partial t^2}\Phi=0. \quad (14)$$

In Fourier space, neglecting the third harmonics (rotating wave approximation), the following wave equation for the slowly varying envelope $\hat{q}(x,\omega-\omega_0)$ can be derived:

$$\frac{\partial^2}{\partial x^2}\hat{q}(\omega-\omega_0)+\epsilon(\omega)\frac{\omega^2}{c^2}\hat{q}(\omega-\omega_0)=0, \quad (15)$$

where the dielectric function

$$\epsilon(\omega)=1+\hat{\chi}^{(1)}(\omega)+\tfrac{3}{4}\hat{\chi}^{(3)}(\omega-\omega_0)aE_0^2|q|^2. \quad (16)$$

The dispersion relation takes the form

$$\epsilon(\omega)\omega^2/c^2=k^2. \quad (17)$$

Its real and imaginary parts are related to the refractive index $n(\omega)$ and the absorption loss coefficient $\alpha(\omega)$ through the relationship

$$\epsilon(\omega)=\left[n(\omega)+i\alpha(\omega)\frac{c}{2\omega}\right]^2. \quad (18)$$

Therefore,

$$n(\omega)=n_0(\omega)+n_2E_0^2|q|^2,$$
$$\alpha(\omega)=\alpha_0(\omega)+\alpha_2(\omega-\omega_0)E_0^2|q|^2, \tag{19}$$

where the linear and nonlinear induced refractive indices are given by

$$n_0(\omega)=\mathrm{Re}[\sqrt{1+\hat{\chi}^{(1)}(\omega)}],$$
$$n_2=\frac{3a\hat{\chi}^{(3)}(0)}{8n_0(\omega_0)}=\frac{3a}{8n_0}, \tag{20}$$

while the single- and two-photon absorption coefficients are

$$\alpha_0(\omega)=\frac{\omega_0}{n_0(\omega_0)c}\mathrm{Im}[\hat{\chi}^{(1)}(\omega)],$$
$$\alpha_2(\omega-\omega_0)=\frac{\omega_0}{n_0(\omega_0)c}\mathrm{Im}[\hat{\chi}^{(3)}(\omega-\omega_0)]. \tag{21}$$

The triple-resonance Lorentz linear dipole oscillators obey a set of three coupled harmonic ordinary differential equations (ODE's),

$$\frac{\partial^2}{\partial t^2}\Phi_j+2\gamma_j\frac{\partial}{\partial t}\Phi_j+\omega_j^2\Phi_j=\beta_j\omega_j^2E, \tag{22}$$

and the Debye electronic relaxation satisfies the following ODE:

$$\frac{\partial}{\partial t}Q+\frac{1}{\tau}Q=\frac{1}{\tau}E^2. \tag{23}$$

The ODE's (22) and (23) are coupled simultaneously to Maxwell's partial differential equations (PDE's) (9), and the full system is solved using a standard FDTD scheme based on the Yee method [13]. The numerical dispersion inherent in these methods has been analyzed in detail [21], and we chose our discretization accordingly.

III. SHOCKS ON THE OPTICAL CYCLE OF ULTRASHORT PULSES

Before considering the numerical solution of the set of equations (9), (22), and (23), it is instructive to consider the dispersionless case by setting $\Phi^{(1)}=0$ and the instantaneous nonlinear response limit $\tau\to 0$. Equation (14) then becomes

$$\frac{\partial^2E}{\partial t^2}-c^2\frac{\partial^2E}{\partial x^2}+a\frac{\partial^2E^3}{\partial t^2}=0. \tag{24}$$

In close connection to Eq. (24) are the one-way wave equations

$$\sigma(E)\frac{\partial E}{\partial t}+\frac{\partial E}{\partial x}=0,$$
$$\sigma(E)=-(1/c)\sqrt{1+3aE^2}. \tag{25}$$

This last nonlinear hyperbolic equation can be solved analytically by the method of the characteristics and admits shock solutions [22]. First, note that Eqs. (25) satisfy the 1D conservation laws

$$\frac{\partial\rho(E)}{\partial t}+\frac{\partial E}{\partial x}=0,$$
$$\rho(E)=\int\sigma(E)dE, \tag{26}$$

subject to the initial data

$$E(x=0,\tilde{t})=f(\tilde{t}) \tag{27}$$

(throughout this paper we use the expression ''initially'' in this sense, i.e., the condition at $x=0$). Recognizing that the differentiation in Eqs. (25) may be written as

$$\frac{d}{dx}=\frac{dt}{dx}\frac{\partial}{\partial t}+\frac{\partial}{\partial x}, \tag{28}$$

which is a directional derivative along the characteristic curves $\mathcal{C}$ given by integrating

$$\mathcal{C}:\frac{dt}{dx}=\sigma(E), \tag{29}$$

which enables Eqs. (25) to be written

$$\frac{dE}{dx}=0 \quad \text{along the characteristics } \mathcal{C}. \tag{30}$$

Thus characteristics transport along them constant values of the solution E and they are nonparallel straight lines [$\sigma(E)\neq\text{const}$] of slope given by Eq. (29). It follows that different elements of the initial wave (27) will propagate at different speeds, so that the wave will reshape with propagation distance x. When $\sigma'(E)>0$, higher values of E propagate faster than lower ones, while when $\sigma'(E)<0$ higher values of E propagate slower and the nonlinear distortion occurs toward the trailing side of the wave. For $\sigma'(E)=0$ (i.e., the linear case), σ is a constant, characteristics are parallel straight lines, and the wave is translated without any change in shape. Nonuniqueness of the solution results when for $x>0$ the characteristics intersect. At some distance a discontinuity or shock forms due to the crossing of two characteristics. This crossing distance is found as follows. Consider two characteristics $\mathcal{C}_1$ and $\mathcal{C}_2$, through the points ($x=0$, $t=\tilde{t}_1$) and ($x=0$, $t=\tilde{t}_2$), respectively. They have the equations

$$\mathcal{C}_1: t=\tilde{t}_1+F(\tilde{t}_1)x,$$
$$\mathcal{C}_2: t=\tilde{t}_2+F(\tilde{t}_2)x, \tag{31}$$

where $F(\tilde{t})=\sigma(f(\tilde{t}))$. The characteristics that cross first must be initially adjacent so that we can take the limit $\tilde{t}_1\to\tilde{t}_2$ to obtain

$$x_B = \lim_{\tilde{t}_1 \to \tilde{t}_2} \frac{\tilde{t}_1 - \tilde{t}_2}{F(\tilde{t}_2) - F(\tilde{t}_1)} = \frac{-1}{F'(\tilde{t}_B)}. \tag{32}$$

Therefore, the smallest breaking distance occurs on the characteristic passing through the point $(x=0,\ \tilde{t}_B)$ for which $F'(\tilde{t}_B)$ is most negative. The solution of Eqs. (25) can then be written in implicit form (for the boundary condition of an input pulse varying in time at $x=0$) by the set of equations

$$\begin{aligned} E(x,t) &= f(x=0,\tilde{t}), \\ \tilde{t} &= t - \sigma(E(x=0,\tilde{t})), \end{aligned} \tag{33}$$

or, equivalently,

$$E(x,t) = f(t - \sigma(E)x) = f(\tilde{t}). \tag{34}$$

Differentiating Eq. (34) yields

$$\begin{aligned} \frac{\partial E}{\partial t}(\tilde{t}) &= f'(\tilde{t})\frac{\partial \tilde{t}}{\partial t} = \frac{f'(\tilde{t})}{1 + F'(\tilde{t})x}, \\ \frac{\partial E}{\partial x}(\tilde{t}) &= f'(\tilde{t})\frac{\partial \tilde{t}}{\partial x} = \frac{-f'(\tilde{t})F(\tilde{t})}{1 + F'(\tilde{t})x}. \end{aligned} \tag{35}$$

Clearly, these derivatives become infinite at the shock location, i.e., when F' achieves its most negative value.

As illustrative example, we have chosen an initial hyperbolic secant soliton pulse

$$E(x=0,t) = E_0 \,\mathrm{sech}(t/t_0)\cos(\omega_0 t). \tag{36}$$

Inserting this initial condition into Eq. (32) yields

$$\begin{aligned} x_B &= (ct_0)\frac{2\sqrt{1 + (3/2)aE_0^2 \,\mathrm{sech}^2[T_0/(8t_0)]}}{aE_0^2 \,\mathrm{sech}^2[T_0/(8t_0)]3\{\tanh[T_0/(8t_0)] + \omega_0 t_0\}}, \\ &\simeq (ct_0)\frac{2\sqrt{1 + (3/2)aE_0^2}}{aE_0^2 3\omega_0 t_0} \quad (T_0 \leqslant t_0) \\ &\simeq \frac{cT_0}{\pi 3aE_0^2}. \end{aligned} \tag{37}$$

The shock distance is thus directly related to the frequency of the third-harmonic generated by the nonlinearity. In the present case $aE_0^2 = 0.06$ (which corresponds to $\delta n = 1.5\%$), $\tau_p/T_0 = 2$ (two-cycle initial pulse), yielding $x_B \sim 1.53ct_0$. For physical reasons the electromagnetic fields must be single valued, therefore when breaking occurs Eqs. (25) must cease to be a valid description of the electromagnetic shocks. In fact, before x_B the pulse bandwidth will have become large enough that dispersion can no longer be neglected.

To calculate the steepening of the pulse *envelope*, Eq. (1) can be used in the dispersionless and instantaneous nonlinear response limits, i.e.,

$$i\frac{\partial A}{\partial x} + i\beta_1 \frac{\partial A}{\partial t} + \gamma\left(1 + \frac{i}{\omega_0}\frac{\partial}{\partial t}\right)|A|^2 A = 0. \tag{38}$$

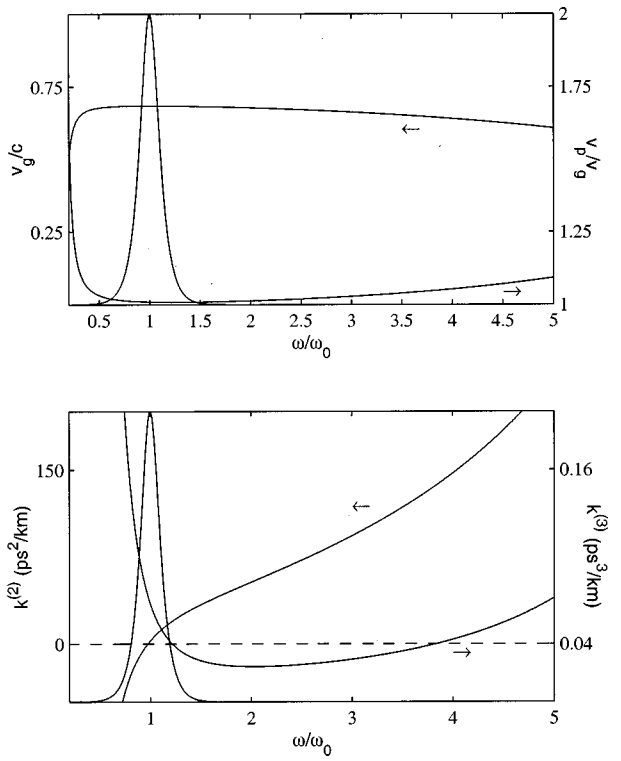

FIG. 1. Bulk fused silica chromatic dispersion. The material parameters are $\beta_1 \sim 0.7$, $\lambda_1 \sim 0.068\,\mu$m, $T_1 = \lambda_1/c \sim 0.22$ fs, $\beta_2 \sim 0.4$, $\lambda_2 \sim 0.116\,\mu$m, $T_2 = \lambda_2/c \sim 0.39$ fs, $\beta_3 \sim 0.9$, $\lambda_3 \sim 9.9\,\mu$m, and $T_3 = \lambda_3/c \sim 33$ fs, where $\lambda_j = 2\pi c/\omega_j$. We have chosen long resonance relaxation times $\gamma_j^{-1} = 5\,\mu$s. The top picture shows the group velocity together with the ratio phase-group velocity. Bottom picture displays group velocity dispersion (GVD) and third order dispersion (TOD). On both pictures we have superimposed the initial pulse spectrum for comparison.

Denoting $s = \gamma/\omega_0 = n_2/c$ and $A = E_0 q \exp(i\varphi(x,t))$, we obtain the following nonlinear hyperbolic equation for the real amplitude q in the group velocity frame of reference:

$$\frac{\partial q}{\partial x} + 3sE_0^2 q^2 \frac{\partial q}{\partial t} = 0. \tag{39}$$

For $q(x=0,t) = \mathrm{sech}(t/t_0)$, we obtain the envelope shocking distance

$$x_B^{\mathrm{env}} \simeq \frac{0.43ct_0}{n_2 E_0^2} = \frac{0.43ct_0}{\delta n} = \frac{8n_0}{3aE_0^2}0.43ct_0, \tag{40}$$

which is proportional to the pulse duration (expressed in units of ct_0). For the initial condition (36), the ratio of the envelope-to-carrier shocking distance is given by

$$\frac{x_B^{\mathrm{env}}}{x_B} \simeq 2\pi n_0 \left(\frac{\tau_p}{T_0}\right), \tag{41}$$

where τ_p is the envelope FWHM. In our case $\delta n = 0.015$, and we obtain $x_B^{\mathrm{env}} \sim 28.6ct_0$ ($x_B^{\mathrm{env}}/x_B \sim 18.7$). Figure 1 shows typical theoretical material chromatic dispersion obtained from the Sellmeier relation (12) valid far from the resonances. For bulk fused silica the parameters are found to be [19] $\beta_1 \sim 0.7$, $\lambda_1 \sim 0.068\,\mu$m, $T_1 = \lambda_1/c \sim 0.22$ fs,

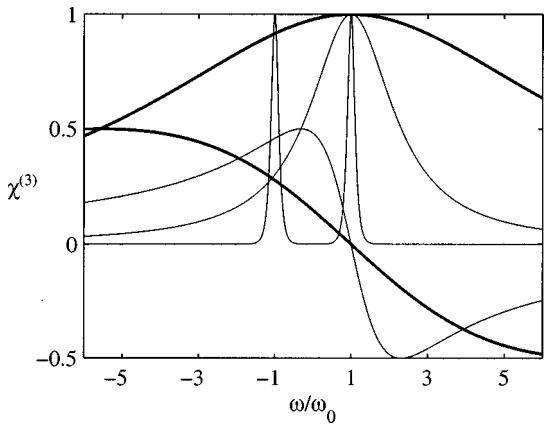

FIG. 2. Theoretical spectrum of the nonlinear electronic susceptibility $\hat{\chi}^{(3)}$. Thick (fine) curves correspond to a relaxation time $\tau = 0.1$ (0.5) fs. Symmetric bell shaped spectra are for the real part of $\hat{\chi}^{(3)}(\omega)$ (related to the nonlinear part of the index of refraction). Antisymmetric spectra are for the imaginary part of $\hat{\chi}^{(3)}(\omega)$ (related to the nonlinear absorption). We have superimposed the initial pulse spectrum for comparison.

$(\omega_1/\omega_0 \sim 18.2)$, $\beta_2 \sim 0.4$, $\lambda_2 \sim 0.116\,\mu$m, $T_2 = \lambda_2/c \sim 0.39$ fs, $(\omega_2/\omega_0 \sim 10.7)$, $\beta_3 \sim 0.9$, $\lambda_3 \sim 9.9\,\mu$m, $T_3 = \lambda_3/c \sim 33$ fs, and $(\omega_3/\omega_0 \sim 0.12)$, where $\lambda_j = 2\pi c/\omega_j$. We have chosen long resonance relaxation times $\gamma_j^{-1} = 5\,\mu$s $[\gamma_j t_0 = 10^{-9}]$. The three absorption bands of SiO_2 are $[\omega_j, \omega_j\sqrt{1+\beta_j}]$. The zero dispersion point (at the inflection point in the index of refraction) $\lambda_{ZDP} \sim 1.27\,\mu$m lies between λ_2 and $\lambda_3/\sqrt{1+\beta_3}$. At the carrier vacuum wavelength $\lambda_0 = 1.24\,\mu$m GVD is only $k^{(2)} \sim 2.83\,\text{ps}^2/\text{km}$. In Fig. 2, the spectrum of the electronic nonlinear susceptibility is displayed together with the initial pulse spectrum. We note the strong nonlinear absorption and the reduction of the effective nonlinear index at the third-harmonic frequency (a nearly 75% reduction in n_2 when $\tau = 0.5$ fs compared to the instantaneous case) due to the finite electronic relaxation on the sub-fs time scale. The slope of absorption curves at $\omega = \omega_0$ is equal to the relaxation time τ. Thick (fine) curves correspond to $\tau = 0.1$ (0.5) fs. Figure 3 displays snapshots at $x = 2.5ct_0$ and $5ct_0$ of the electric optical cycle for an ideal nonlinear dispersionless medium. Calculated shocking dis-

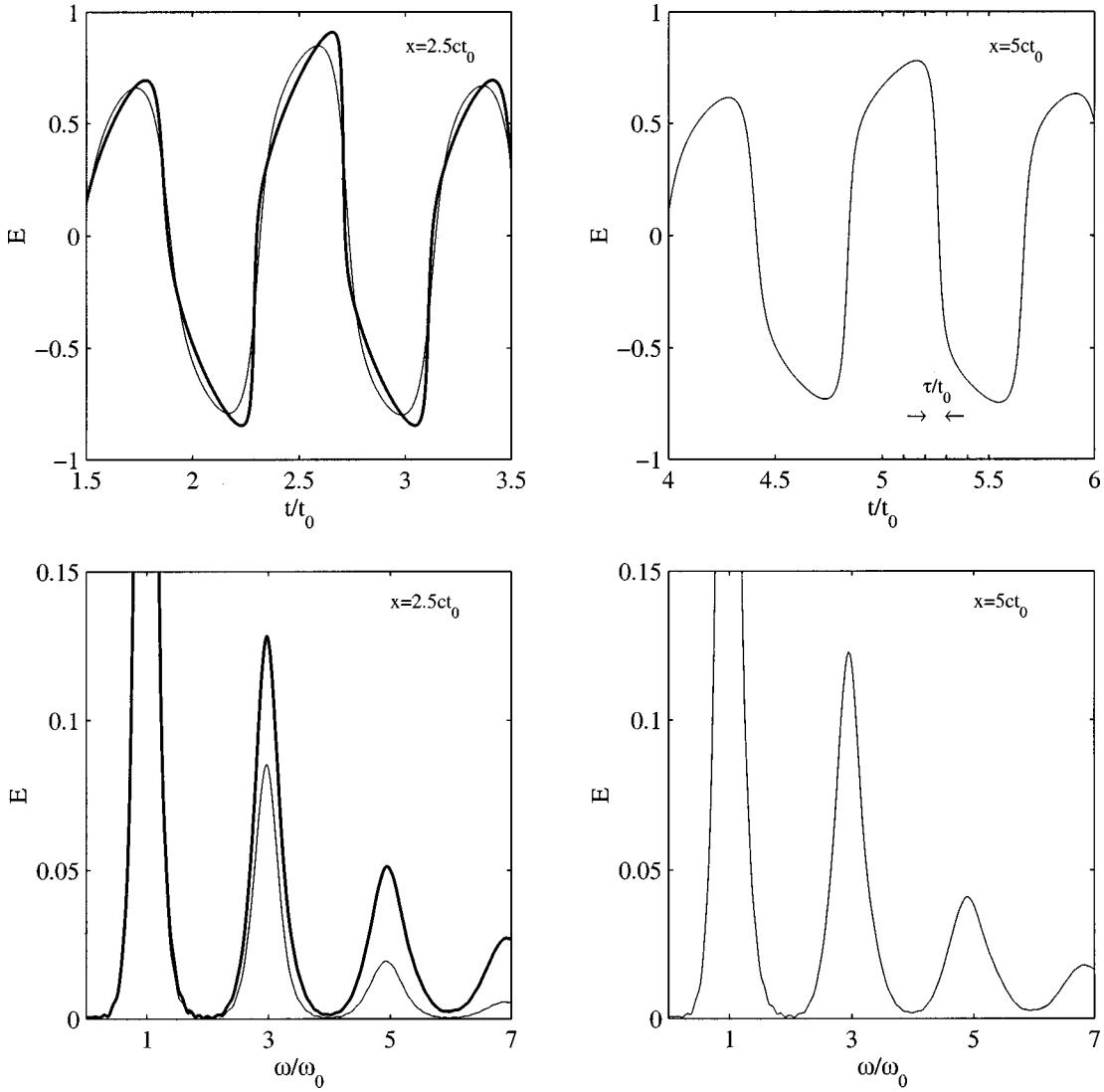

FIG. 3. Evolution of an initial sech of duration $\tau_p = 8.8$ fs ($t_0 = 5$ fs), vacuum carrier wavelength $\lambda_0 = 1.24\,\mu$m ($\tau_p/T_0 \sim 2$) in an ideal nonlinear dispersionless medium. Thick (fine) optical cycles correspond to a relaxation time of $\tau = 0.1$ (0.5) fs. Snapshots are taken at $x = 2.5ct_0$ and $x = 5ct_0$. Bottom figures are the corresponding spectra.

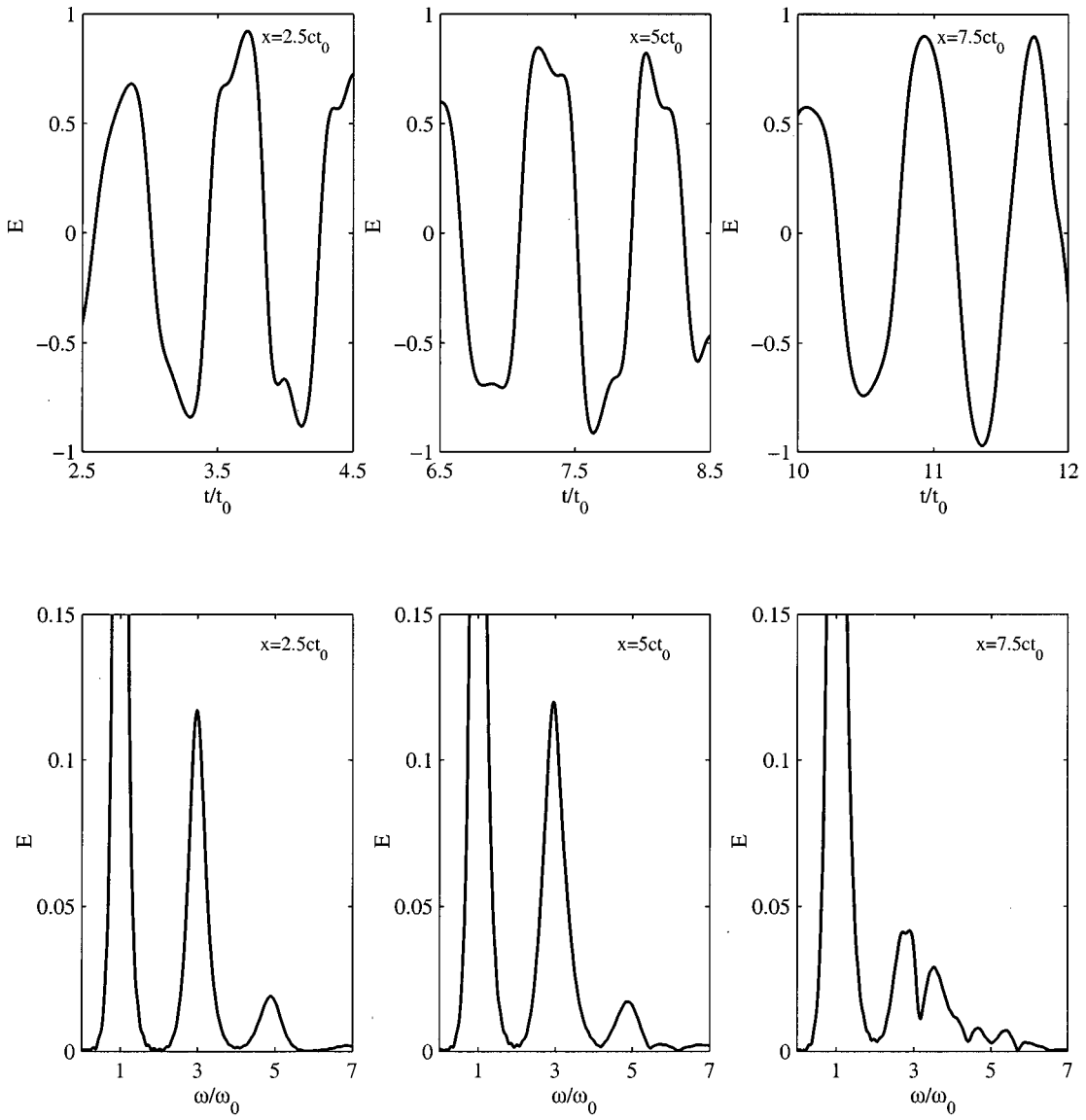

FIG. 4. Evolution of an initial sech pulse of duration $\tau_p = 8.8$ fs, ($t_0 = 5$ fs), vacuum carrier wavelength $\lambda_0 = 1.24\ \mu$m ($\tau_p / T_0 \sim 2$) in bulk fused silica (material parameters given in Fig. 1 with a GVD of 2.83 ps^2/km. All plots are for an instantaneous nonlinear response. Snapshots are taken at $x/(ct_0) = 2.5$, 5, and 7.5 showing the shocks on the modulation cycle.

tance for an infinitely fast response of the nonlinear polarization is $x_B \sim 1.53ct_0$. Numerical results indicate clearly that the finite relaxation time of the nonlinear electronic response (sub-fs time scale) (i) slows down the steepening rate of the optical cycle, (ii) does not limit the generation of strongly phase matched optical harmonics and consequently the development of infinitely sharp edges on the the optical cycle producing its breaking when linear dispersion is not included. Even for a very fast relaxation of 0.1 fs, shocks on the optical cycle only appear for $x \geqslant 2.5ct_0$, and when $\tau = 0.5$ fs after $x \geqslant 5ct_0$. Since $\sigma'(E) < 0$ high intensity parts of the optical cycle propagate slower than low intensity ones. The finite relaxation time of the electronic nonlinearity does not limit the generation of phase-matched harmonics and therefore steepening on the optical cycle when dispersion and losses are neglected. Equal steepening on both the front and back edges of the modulation cycle is observed. In the limit of an instantaneous intensity dependent index of refraction, a sharp jump on the optical cycle occurs at $x_B \sim 1.5ct_0$ and our numerical algorithm breaks down at larger distances in that case. Dispersion prevents the development of an infinitely sharp jump and hence limits the frequency spectrum of the harmonics generated. Figure 4 shows the optical cycle near the zero-dispersion point of bulk fused silica for a zero-relaxation time limit. Note that the third-harmonic peak is nearly as strong as in the dispersionless, non-zero-relaxation time limit, but the higher harmonics are not phase matched and much weaker. At $x = 7.5ct_0 \sim 0.9L_{\mathrm{NL}} \sim 0.26x_B^{\mathrm{env}}$, the instantaneous nonlinearity (self-phase modulation) leads to sprectral broadening and modulation, which indicates the development of steepening on the pulse envelope. Finally, in Fig. 5, the effect of a finite relaxation time is taken into account. For a relaxation time equal to $\tau = 0.1$ fs, a reduction in the production of harmonics of $\sim 15\%$ is observed compared to the zero-relaxation time limit. When $\tau = 0.5$ fs, a reduction of nearly $\sim 40\%$ is ob-

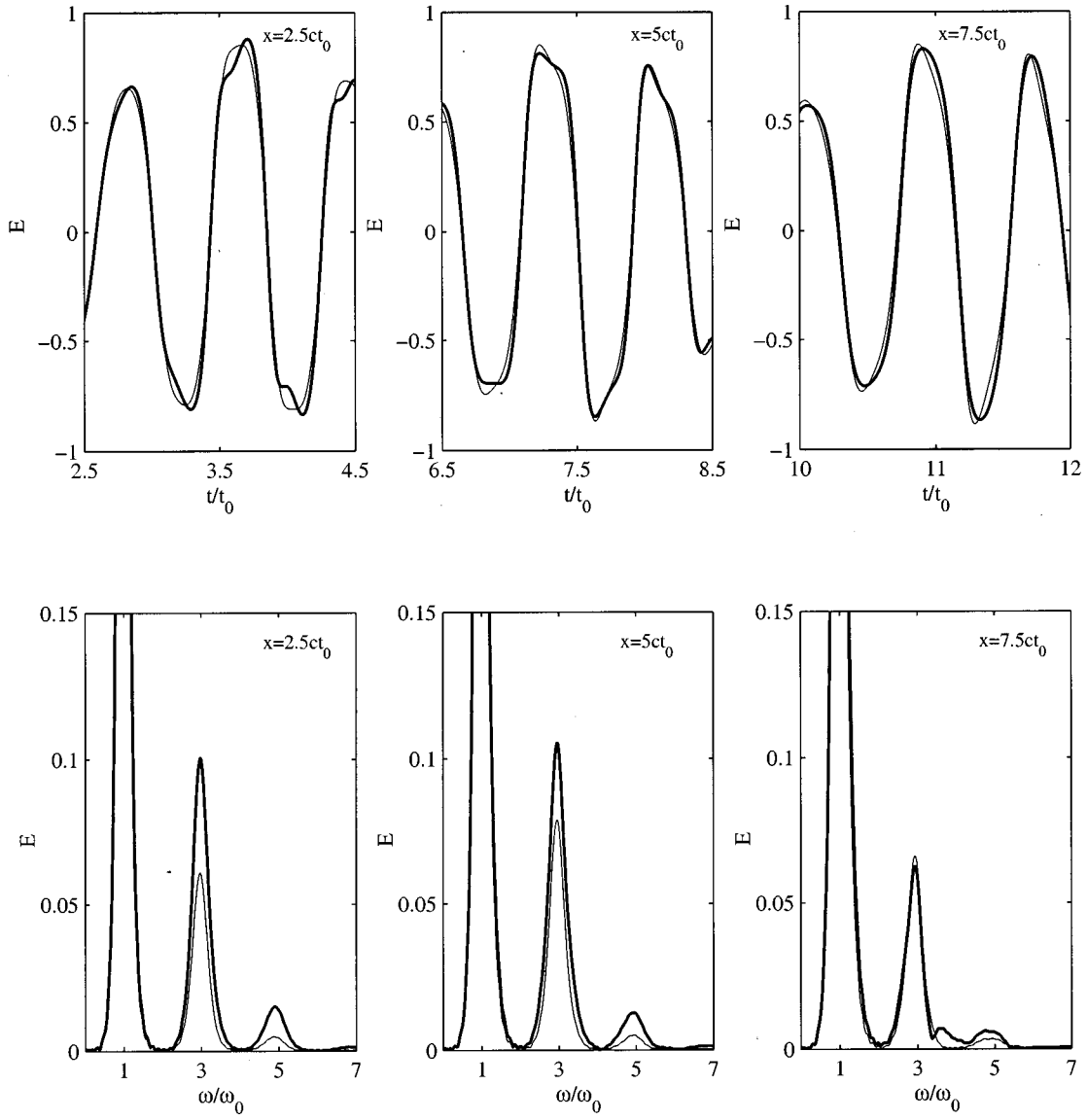

FIG. 5. Evolution of an initial sech pulse of duration $\tau_p = 8.8$ fs ($t_0 = 5$ fs), vaccum carrier wavelength $\lambda_0 = 1.24\,\mu$m ($\tau_p/T_0 \sim 2$) in bulk fused silica (material parameters are given in Fig. 1 with a GVD of 2.83 ps^2/km. Thick (fine) optical cycles correspond to a relaxation time of $\tau = 0.1$ (0.5) fs. Snapshots are taken at $x/(ct_0) = 2.5$, 5, and 7.5 showing the shocks on the modulation cycle.

served. Relaxation on the sub-fs time scale can thus markedly increase the thickness of the shocks (reduces the steepness) on the optical cycle in dispersive media. Note the absence of broadening and modulation of the harmonic spectrum in contrast to the infinitely fast electronic response limit.

IV. CONCLUSIONS

In conclusions, using the FDTD method, recently applied to the field of nonlinear optics [13], from the full Maxwell's equations we have illustrated the effects of a finite nonlinear electronic response time (sub-fs time scale) on the formation of electromagnetic shocks on the optical optical of a sub-10-fs two-cycle ultrashort pulse linearly polarized with a carrier wavelength of $\lambda_0 = 1.24\,\mu$m traveling in the normal dispersion region of a third-order triple-resonance Lorentz transparent medium. For illustrative purposes we have chosen fused silica (SiO_2) as the host material due to its considerable importance in optical communications and good dispersive properties around the zero-dispersion point. Formation of electromagnetic shocks on the modulation cycle, directly related to the generation of optical harmonics, has been proven, as conjectured by Rosen [16] in 1965, and recently reconsidered in Ref. [17] for a single-resonance Lorentz medium with instantaneous nonlinear response. Numerical results indicate that the finite relaxation time of the nonlinear electronic response (sub-fs time scale) (i) slows down the steepening rate of the optical cycle; (ii) does not limit the generation of strongly phase matched optical harmonics and consequently the development of infinitely sharp edges on the the optical cycle producing its breaking when linear dis-

persion is not included; (iii) reduces the production of phase matched harmonics and consequently the sharpening of the jumps when dispersion is present, compared to the case of an instantaneous nonlinear response; and (iv) reduces the harmonic spectrum spreading and modulation at later times on the appearance of self-steepening of the electric field envelope. Interferometric fringe autocorrelation techniques may provide direct measurement of the optical cycle [18] and thus carrier shock formation.

ACKNOWLEDGMENTS

L.G. is grateful to the Comunidad Autonoma de Madrid for a research grant, and to the Arizona Center for Mathematical Sciences (ACMS), where part of this work was carried out. L.V. thanks the Comisión Interministerial de Ciencia y Tecnología of Spain (Grant No. PB95-0426) for partial support. We are grateful to M. Mlejnek for his interest on this problem.

[1] G. P. Agrawal, *Nonlinear Fiber Optics* (Academic, New York 1995).

[2] P. F. Curley, Ch. Spielmann, T. Brabec, F. Krausz, E. Wintner, and A. J. Schmidt, Opt. Lett. **18**, 54 (1993); J. Zhou, G. Taft, C.-P. Huang, M. M. Murname, and H. C. Kapteyn, *ibid.* **19**, 1149 (1994); M. Nisoli, S. De Silvestri, O. Svelto, R. Szipöcs, K. Ferencz, Ch. Spielmann, S. Sartania, and F. Krausz, *ibid.* **22**, 522 (1997).

[3] B. Kohler, V. V. Yakovlev, J. Che, J. L. Krause, M. Messina, K. R. Wilson, N. Schwentner, R. M. Whitnell, and Y. Yan, Phys. Rev. Lett. **74**, 3360 (1995).

[4] B. B. Hu and M. C. Nuss, Opt. Lett. **20**, 1716 (1995).

[5] T. Brabec and F. Krausz, Phys. Rev. Lett. **78**, 3282 (1997).

[6] K. J. Blow and D. Wood, IEEE J. Quantum Electron. **25**, 2665 (1989).

[7] R. W. Hellwarth, A. Owyoung, and N. George, Phys. Rev. A **4**, 2342 (1971).

[8] J. P. Gordon, Opt. Lett. **11**, 662 (1986).

[9] F. M. Mitschke and L. F. Mollenauer, Opt. Lett. **11**, 659 (1986).

[10] J. R. Taylor, *Optical Solitons, Theory and Experiment* (Cambridge University Press, Cambridge, 1992).

[11] L. Gilles, H. Bachiri, and L. Vázquez, Phys. Rev. E **57**, 6079 (1998).

[12] K. L. Shlager and J. B. Schneider, IEEE Antennas Propag. Mag. **37**, 39 (1995).

[13] A. Taflove, *Computational Electrodynamics: The Finite-Difference Time-Domain Method* (Artech House, Norwood, 1995); A. Taflove, *Advances in Computational Electrodynamics: The Finite-Difference Time-Domain Method* (Artech House, Norwood, 1998); K. S. Kunz and R. J. Luebbers, *The Finite Difference Time Domain Method for Electromagnetics* (CRC Press, Boca Raton, FL, 1993).

[14] G. P. Agrawal and C. Headley III, Phys. Rev. A **46**, 1573 (1992); Y. S. Kivshar and B. A. Malomed, Opt. Lett. **18**, 485 (1993).

[15] D. Cai, A. R. Bishop, N. G.-Jensen, and B. A. Malomed, Phys. Rev. Lett. **78**, 223 (1997).

[16] G. Rosen, Phys. Rev. **139**, A539 (1965).

[17] R. G. Flesch, A. Pushkarev, and J. V. Moloney, Phys. Rev. Lett. **76**, 2488 (1996).

[18] P. F. Curley, Ch. Spielmann, T. Brabec, F. Krausz, E. Winter, and A. J. Schmidt, Opt. Lett. **18**, 54 (1993); A. Stingl, M. Lenzner, Ch. Spielmann, F. Krausz, and R. Szipöcs, Opt. Lett. **20**, 602 (1995).

[19] I. H. Malitson, J. Opt. Soc. Am. **55**, 1205 (1965).

[20] P. N. Butcher and D. Cotter, *The Elements of Nonlinear Optics* (Cambridge University Press, Cambridge, 1990).

[21] P. G. Petropoulos, IEEE Trans. Antennas Propag. **42**, 62 (1994); **42**, 859 (1994).

[22] G. B. Whitham, *Linear and Nonlinear Waves* (Wiley, New York, 1974); T. Taniuti and K. Nishihara, *Nonlinear Waves* (Pitman, Boston, 1983).